Arch Iran Med. February 2021;24(2):144-151

doi 10.34172/aim.2021.23

http://www.aimjournal.ir

ARCHIVES OF IRANIAN MEDICINE

Open Access

Original Article

Post-mortem Histopathologic Findings of Vital Organs in Critically Ill Patients with COVID-19

Farahnaz Bidari Zerehpoosh, MD[1]; Shahram Sabeti, MD[1]; Hooman Bahrami-Motlagh, MD[2]; Majid Mokhtari, MD[3]; Seyed Sina Naghibi Irvani, MD[4]; Parham Torabinavid, MD[4]; Farzad Esmaeili Tarki, MD[4]; Mahdi Amirdosara, MD[5]; Omidvar Rezaei, MD[6]; Babak Mostafazadeh, MD[7,8]; Mohammadreza Hajiesmaeili, MD[5]; Mohammad Mahdi Rabiei, MD[4]; Ilad Alavi Darazam, MD[4,9*]

[1]Department of Pathology, Loghman Hakim Hospital, Shahid Beheshti University of Medical Sciences, Tehran, Iran
[2]Department of Radiology, Loghman Hakim Hospital, Shahid Beheshti University of Medical Sciences, Tehran, Iran
[3]Department of Pulmonary and Critical Care Medicine, Loghman Hakim Hospital, Shahid Beheshti University of Medical Sciences, Tehran, Iran
[4]Department of Infectious Diseases and Tropical Medicine, Loghman Hakim Hospital, Shahid Beheshti University of Medical Sciences, Tehran, Iran
[5]Anesthesiology Research Center, Loghman Hakim Hospital, Shahid Beheshti University of Medical Sciences, Tehran, Iran
[6]Skull Base Research Center, Loghman Hakim Hospital, Shahid Beheshti University of Medical Sciences, Tehran, Iran
[7]Department of Forensic Medicine, School of Medicine, Shahid Beheshti University of Medical Sciences, Tehran, Iran
[8]Toxicological Research Center, Shahid Beheshti University of Medical Sciences, Tehran, Iran
[9]Infectious Diseases and Tropical Medicine Research Center, Shahid Beheshti University of Medical Sciences, Tehran, Iran

Abstract

Background: The scientific evidence concerning pathogenesis and immunopathology of the coronavirus disease 2019 (COVID-19) is rapidly evolving in the literature. To evaluate the different tissues obtained by biopsy and autopsy from five patients who expired from severe COVID-19 in our medical center.

Methods: This retrospective study reviewed five patients with severe COVID-19, confirmed by reverse transcription-polymerase chain reaction (RT-PCR) and imaging, to determine the potential correlations between histologic findings with patient outcome.

Results: Diffuse alveolar damage (DAD) and micro-thrombosis were the most common histologic finding in the lung tissues (4 of 5 cases), and immunohistochemical (IHC) findings (3 of 4 cases) suggested perivascular aggregation and diffuse infiltration of alveolar walls by CD4+ and CD8+ T lymphocytes. Two of five cases had mild predominantly perivascular lymphocytic infiltration, single cell myocardial necrosis and variable interstitial edema in myocardial samples. Hypertrophic cardiac myocytes, representing hypertensive cardiomyopathy was seen in one patient and CD4+ and CD8+ T lymphocytes were detected on IHC in two cases. In renal samples, acute tubular necrosis was observed in 3 of 5 cases, while chronic tubulointerstitial nephritis, crescent formation and small vessel fibrin thrombi were observed in 1 of 5 samples. Sinusoidal dilation, mild to moderate chronic portal inflammation and mild mixed macro- and micro-vesicular steatosis were detected in all liver samples.

Conclusion: Our observations suggest that clinical pathology findings on autopsy tissue samples could shed more light on the pathogenesis, and consequently the management, of patients with severe COVID-19.

Keywords: Autopsy, COVID-19, Diffuse alveolar damage, Pneumonia, SARS-CoV-2, Thrombosis

Cite this article as: Bidari Zerehpoosh F, Sabeti S, Bahrami-Motlagh H, Mokhtari M, Naghibi Irvani SS, Torabinavid P, et al. Post-mortem histopathologic findings of vital organs in critically Ill patients with COVID-19. Arch Iran Med. 2021;24(2):144–151. doi: 10.34172/aim.2021.23.

Received: October 7, 2020, Accepted: November 16, 2020, ePublished: February 1, 2021

Introduction

As of May 20, 2020, the coronavirus disease 2019 (COVID-19), a pandemic infection caused by severe acute respiratory syndrome coronavirus 2 (SARS-CoV-2), has accounted for 318789 deaths from 4789205 confirmed cases globally.[1]

Although the majority of COVID-19 patients develop only mild to moderate symptoms, progressive pneumonia and subsequent acute respiratory distress syndrome (ARDS) and multi-organ failure occur in a significant number of patients.[2]

Evidence concerning the pathogenesis and other aspects of COVID-19 immunopathology was limited at the onset of the outbreak. Gradually, some preliminary studies were able to identify new characteristics of the disease in seriously ill hospitalized patients. However, similarities between COVID-19 and severe acute respiratory syndrome (SARS), in terms of pathological, clinical, and pathogenic characteristics, have aided us to gain a better understanding of the pathogenesis of this disease.[3]

The SARS-CoV-2 infection can trigger both the innate and the adaptive immune pathways. Nevertheless, uninhibited innate reactions along with a disrupted adaptive immune response can ultimately trigger

***Corresponding Author:** Ilad Alavi Darazam, MD; Department of Infectious Diseases and Tropical Medicine, Shahid Beheshti University of Medical Sciences, Kargar Ave., Tehran 1333635445, Iran. Tel: +98 21 5541 9005; Email: ilad.alavi@sbmu.ac.ir & ilad13@yahoo.com

devastating tissue damage. In patients with severe COVID-19, the expression of the CD94/NK group 2 member A (NKG2A), an exhaustion marker on NK cells, and CD8 + T cells are increased and their normalization is associated with improved CD4 + T cells, CD8 + T cells, B cells and NK cells as well as fatigue markers, during the recovery and improvement phase.[2]

In addition to elevated levels of pro-inflammatory cytokines, plasma concentrations of interleukin (IL)-2, IL-7, IL-10, granulocyte-colony stimulating factor, interferon gamma-induced protein 10, monocyte chemo-attractant protein-1, macrophage inflammatory protein 1-a and tumor necrosis factor-alpha in critically ill COVID-19 patients display greater levels compared to those with mild to moderate disease.[4]

Also, it has been established that there is a direct relationship between high levels of pro-inflammatory cytokines and end-organ damage and failure of the heart, liver, kidneys and lungs.[2]

Recently, a few studies on histopathologic aspects of fatal COVID-19 have been published in the literature.[5-7] In addition to the pathological findings compatible with ARDS, other investigators have reported some histological features which tend to be different from the classic cases of ARDS.[5]

In addition, endothelial disruption observed in tissues such as the kidneys, intestines and the scalp, indicate the impact of virus-induced vascular impairment during disease progression.[6]

Despite the recent efforts in understanding the pathogenesis of the COVID-19, we are still at the early stages of elucidating the various aspects of this disease and studies carried out so far suggest significant clinical and histopathologic variability exhibited by COVID-19.[7]

Therefore, there is an urgent need to acquire precise and robust data to explain the immunopathogenesis of the COVID-19 and its impact on the human body.

In this investigation, we aimed to examine a variety of organs, including the lung, kidney, heart and liver, obtained from several fatal cases of COVID-19, in order to have a more clear understanding of the pathogenesis of this disease.

Materials and Methods

Five patients who died of severe COVID-19 in the intensive care unit (ICU) were selected by an infectious disease specialist (IAD) and critical care specialist (MA) for the study. The patients had diffuse pulmonary infiltrates compatible with COVID-19 pneumonitis on their computed tomography (CT) scans, oxygen saturation (SpO_2) <93% in ambient air and/or respiratory rate >24/minute with confirmation of their disease by reverse transcription-polymerase chain reaction (RT-PCR).

All necropsies were performed immediately after the declaration of death by one forensic medicine specialist (BM).

For optimal targeting of the organs, tissue sample were acquired under ultrasound-guidance (MyLab, Esaote, Italy) by a radiologist (HBM) with more than 8 years of experience in ultrasound-guided intervention, utilizing an automatic 14-gauge core biopsy needle (Acecut, TSK Laboratory, Japan).

All postmortem core needle biopsy samples were preserved in 10% neutral buffered formalin and fixed for 72 hours before processing based on the Centers for Disease Control and Prevention recommendations available at: (https://www.cdc.gov/ncezid/dhcpp/idpb/specimen-submission/general-unexplained.html)

All hematoxylin and eosin (H&E), cluster differentiation CD3, CD20, CD4 and CD8 stained biopsy sections and cytomegalovirus (CMV) stained lung and liver biopsy slides, related to cases number 4 and 5, respectively, were examined separately by two pathologists (FBZ, SS).

This study was undertaken at Loghman Hakim hospital, a major affiliate of the Shahid Beheshti University of Medical Sciences in Tehran, Iran between April 2, 2020 and May 10, 2020. Informed consent for the procedure was obtained from the legal guardians of all deceased patients.

Results

Case Presentations

Case 1: A 78-year-old woman with a history of hypertension and hypothyroidism presented to the emergency department (ED) with increasing shortness of breath and respiratory distress. The patient was recently hospitalized with a SARS-CoV-2 RT-PCR positive COVID-19 diagnosis and had received lopinavir/ritonavir. On admission, arterial oxygen saturation on ambient air was 80% and chest CT findings showed bilateral pleural effusion (more so on the right side), right-sided pneumothorax, and diffused patchy ground-glass opacities. A right-sided chest tube was placed, and amikacin and meropenem were started in the ED. She initially responded to supportive care and oxygen therapy but had to be intubated and mechanically ventilated on day 4 of her admission. She developed organ hypoperfusion and severe hypoxia which was unresponsive to the escalation of mechanical ventilation support and vasoactive agents and expired on the same day.

Case 2: A 48-year-old man presented with dyspnea, purulent cough, fever, and chills for the last 7 days. On admission to the ED, he was in respiratory distress, tachycardic, hypotensive, afebrile with SpO_2 of 70% on ambient air. Chest CT findings showed bilateral diffuse patchy ground-glass opacities. Bi-level positive airway pressure (BIPAP) was initiated for the patient. Oxygen

saturation increased to 79% after one hour on BIPAP and then he was intubated immediately. Remdesivir, hydroxychloroquine, ceftriaxone, and azithromycin were started in the ED. On days 5 and 7, the patient received hemoperfusion. On day 8, the patient was intubated and tocilizumab was started on day 9. On day 10, umifenovir and atazanavir were added to his treatment regimen. The patient continued to deteriorate and expired on day 11.

Case 3: A 75-year-old woman with a history of hypertension, ischemic heart disease, cerebrovascular accident, diabetes mellitus, and dyslipidemia presented with fatigue for 3 days before presentation to the ED followed by dyspnea, aphasia and diminished level of consciousness. On admission to the ED, her respiratory rate was 18 per minute, temperature was 36°C, heart rate was 80 per minute and SpO_2 was 50% on ambient air. The CT of the chest and non-contrast head findings were diffused patchy ground-glass opacities and periventricular hypodensities, respectively. Lopinavir/ritonavir, interferon beta-1a and hydroxychloroquine were started in the ED along with supportive care and stepwise oxygen therapy. The patient expired 12 hours after admission.

Case 4: A 71-year-old man presented with dyspnea and fever for the last 14 days, and worsening of symptoms 4 days prior to presentation to the ED. Dyspnea was his first symptom which was followed by fever a week later. He had been admitted to another hospital with confirmed COVID-19 diagnosis on RT-PCR and had received hydroxychloroquine 200 mg twice daily for 72 hours before admission. On admission to the ED, his heart rate was 98 beats per minute, respiratory rate was 18 per minute, the temperature was 38°C, and SpO_2 was 70%. CT scan of the chest illustrated bilateral diffuse patchy ground-glass opacities. Lopinavir/ritonavir, interferon beta-1a and one dose of hydroxychloroquine were administered on admission. On day 3 of his ICU admission, vitamin C 1 gram four times daily was started and non-invasive ventilation was initiated for persistent hypoxia. On day 4, the patient had to be intubated and mechanically ventilated with lung protective strategy and FiO_2 of 100%. The patient continued to deteriorate despite critical care support and administration of tocilizumab and expired on day 7 of his admission.

Case 5: A 47-year-old woman presented to the ED with dyspnea, fever, cough, headache, and dizziness. She had previously been hospitalized with an RT-PCR confirmed diagnosis of COVID-19. On admission to the ED, her temperature was 39.5°C and SpO_2 on ambient air was 70%. Lopinavir/ritonavir, hydroxychloroquine and azithromycin were started on admission day. On day 2, ribavirin was added to the treatment regimen. On day 5, azithromycin was discontinued and interferon beta-1a was started. On day 8, she was mechanically ventilated with a lung-protective strategy. On day 10, lopinavir/ritonavir was omitted and teicoplanin and atazanavir were started. Chest CT on day 13 revealed worsening bilateral diffused patchy ground-glass opacities. She continued to deteriorate till day 22 when she received 3 sessions of hemoperfusion to no avail and died on the same day.

Detailed clinical and laboratory findings of all patients are shown in Table 1.

Histologic Findings

Lung

All samples of lung tissue revealed different stages of diffuse alveolar damage (DAD) in addition to microvascular changes and micro-hemorrhage, detailed below:

Case 1: DAD accompanied by acute exudative pneumonia, likely representing bacterial superinfection.

Case 2: Sample, was not adequate for histopathologic evaluation.

Case 3: Mild mixed exudative-proliferative DAD with delicate hyaline membrane formation, mild interstitial lymphocytic infiltration, pneumocyte necrosis, desquamation, slight hyperplasia of pneumocyte type 2 and small vessels fibrin thrombosis.

Case 4: Severe DAD, with the same features as specimen 5, as well as atypical pneumocytes with large vesicular nuclei, prominent nucleoli and vacuolated cytoplasm (resembling CMV cytopathic effect), focal squamous metaplasia and early fibrosis associated with focal Masson body formation, the latter two adding a fibrotic component to the DAD.

Case 5: Severe mixed exudative-proliferative DAD with severe inflammation, predominantly lymphocytic, admixed with few neutrophils and histiocytes, prominent hyaline membrane formation, fibrin deposition and hemorrhage in alveolar walls and spaces, frequent microthrombi in alveolar capillaries, thickening of small vessel walls, pneumocyte desquamation and diffuse hyperplasia of pneumocyte type 2 (Table 2).

Immunohistochemical (IHC) Findings

Cases 3, 4, and 5: Perivascular aggregation and diffuse infiltration of alveolar walls by CD4+ and CD8+ T lymphocytes and smaller amount of CD20+ B lymphocytes. Case 4 was CMV negative and multinucleated giant cells were stained with TTF1 as it was expected in pneumocytes (Figure 1).

Heart

Cases 1 and 4: Predominantly perivascular mild lymphocytic infiltration, single cell myocardial necrosis and variable interstitial edema.

Cases 2 and 5: Normal myocardial histology.

Case 3: Hypertrophied cardiac myocytes with enlarged

Table 1. The Clinical Characteristics of Patients

Characteristics	Patient-1		Patient-2		Patient-3		Patient-4		Patient-5	
Age	78		48		75		71		47	
Gender	Female		Male		Female		Male		Female	
Previous hospitalization due to COVID-19	Yes		No		No		Yes		Yes	
Therapeutic regimen on previous hospitalization	Lopinavir/ritonavir		—		—		Hydroxychloroquine		—	
Presenting symptoms	ARDS		Dyspnea, cough, sputum		Dyspnea, LOC, aphasia		Dyspnea, fever		Dyspnea, fever, cough, headache, dizziness	
Onset of symptoms	6 days before presentation		7 days before presentation		3 days before presentation		14 days before presentation		4 days before presentation	
LOS-Hospital	4		11		1		7		22	
Days from admission to death	4		11		1		7		22	
Hemoperfusion	—		Yes-2 episode (day 4, 6)		—		—		Yes- DAY 22: 3 episodes	
Therapeutic regimen	Lopinavir/ ritonavir,		Day 0: Remdesivir, Hydroxychloroquine, Day 7: +Tocilizumab DAY 9: +umifenovir (Arbidol) & atazanavir		Interferon beta-1a, hydroxychloroquine, lopinavir/ritonavir		Lopinavir/Ritonavir, Interferon beta-1a, Hydroxychloroquine Day 5: +Tocilizumab		DAY 0: Lopinavir/ ritonavir, hydroxychloroquine, azithromycin, DAY 1: + Ribavirin DAY 6: + Interferon beta-1a DAY 10: -Lopinavir/ ritonavir, + teicoplanin & atazanavir	
Past medical history	HTN, hypothyroidism,		No		IHD, HTN, CVA, DM, DLP, LBBB (ECG)		No		—	
Allergy history	Penicillin		—		—		—		—	
Other therapeutic agents	Meropenem, amikacin		Ceftriaxone, azithromycin		—		DAY 2: Vitamin C		DAY 16: meropenem, colistin, levofloxacin	
O_2 saturation arterial	80		<80		50		70		70	
Laboratory findings	**First**	**Last**	**First**	**Last**	**First**	**Last**	**First**	**Last**	**First**	**Last**
Hb	8.1	7.3	10.9	8.8	12.1	—	14.1	11.7	11.8	8.4
Ferritin	—	851	—	968	—	—	710	689	—	—
WBC	13.5	7.7	11.4	19.2	7.3	—	5.3	8.3	4.6	35.5
Neutrophil	94	94.1	91	93.4	83.6	—	84	90.6	80.6	—
Lymphocyte	3.6	4.5	7	3.8	8.3	—	12.4	6.4	14.6	—
Platelet	93 000	34 000	208 000	48 000	195 000	—	129 000	136 000	174 000	102 000
ESR	48	—	71	—	37	—	45	—	72	—
CRP	87.8	—	61.6	83.7	—	—	48	52.3	46	—
ALT	35	—	35	—	159	—	47	47	66	—
AST	80	—	84	—	148	—	81	91	57	—
Total Bili	1.9	—	1	—	—	—	0.7	1.8	—	—
Direct Bili	0.4	—	0.4	—	—	—	0.2	0.8	—	—
Alkaline phosphatase	375	—	133	—	455	—	123	—	187	—
LDH	—	—	—	—	732	—	917	—	988	—
PT	12.9	14.8	12.5	13.6	14.7	—	12.5	14.4	13.2	17.6
PTT	36	42.4	45	34.1	41.6	—	42.4	39.4	35.8	54.4
INR	1.06	1.38	1	1.17	1.36	—	1	1.31	1.11	—
D-dimer	—	—	0.7	3.41	—	—	3.7	3.67	—	—
Cr	0.8	0.8	1.5	1.5	1.4	—	1.1	1.2	0.9	1.1
Urea	59	66	66	96	64	—	45	95	41	69
PaO_2	89.1	118.6	27.5	41	23.3	—	46	90.7	42.7	29.3
HCO_3	24.2	13.2	29.1	20	19.2	—	24.6	23.9	26.9	27.1
pH	7.50	7.028	7.533	7.101	7.27	—	7.41	7.42	7.459	7.308
Ground-glass opacity	Patchy-diffuse		Patchy-diffuse		Patchy-diffuse		Patchy-diffuse		Patchy-diffuse	
Anatomic sides involved	Bilateral		Bilateral		Bilateral		Bilateral		Bilateral	

ARDS, acute respiratory distress syndrome; LOC, loss of consciousness; LOS, length of stay; ALT, alanine aminotransferase; AST, aspartate aminotransferase; BIPAP, Biphasic Positive Airway Pressure; Ca, calcium; CK-MB, creatine kinase myocardial band; CPK, creatine-phosphokinase; Cr, creatinine; CRP, C reactive protein; CSF, cerebrospinal fluid ; CT, computes tomography; CVA, cerebrovascular accident; ECG, electrocardiogram; ESR, erythrocyte sedimentation rate; Fe, iron; FiO2, Fraction of inspired oxygen; Hb, hemoglobin; HCO3, bicarbonate; Hct, hematocrit; HTN, hypertension; ICU, intensive care unit; INR, international normalized ratio; LDH, Lactate dehydrogenase; MCH, Mean corpuscular hemoglobin; MCHC, mean corpuscular hemoglobin concentration; MCV, mean corpuscular volume; NIV, Non-invasive ventilation; PaCO2, Partial pressure of carbon dioxide; PaO2, Partial pressure of oxygen; PEEP, Positive end-expiratory pressure; PH, potential of hydrogen; PSV, Pressure support ventilation; PT, Prothrombin time; PTT, Partial thromboplastin time; RBC, red blood cell; T4, thyroxine; TSH, thyroid stimulating hormone; WBC, white blood cell.

Table 2. The Histopathologic Features of Patients

	Case 1	Case 2	Case 3	Case 4	Case 5
Lung	Severe DAD; Hemorrhage; Thrombosis; Neutrophilic aggregation with scattered CD4, CD8 and lesser CD20 lymphocytes	Inadequate for evaluation	Hyaline membrane formation; Mild neutrophilic and lymphocytic infiltration; Pneumocyte desquamation and hyperplasia; Vascular microthrombi	Severe DAD with exuberant pneumocyte type2 hyperplasia; Focal squamous metaplasia; Atypical multinucleated giant pneumocytes (TTF1+, CMV negative); Mild fibromuscular hyperplasia and vascular microthrombi	Severe DAD; Moderate interstitial lymphocytic, mostly T cell, infiltration; Thickening of small vessel wall;Vascular microthrombi
Heart	Few interstitial perivascular lymphocytic infiltration; CD4 and CD8 positive infiltration	Unremarkable myocardial tissue	Myocardial hypertrophy with boxcar shaped nuclei	Mild perivascular CD4& CD8 T lymphocytes; Single cell myocardial necrosis	Unremarkable myocardial tissue
Kidney	Tubular atrophy; Moderate interstitial chronic inflammation &fibrosis; Glomerular obsolescence (30% of glomeruli)	Unremarkable renal tissue	Mild tubular atrophy; Mild interstitial inflammation; Glomerular obsolescence (10% of glomeruli); Patchy tubular necrosis	Patchy ATN; Mild interstitial inflammation and fibrosis; Glomerular crescent formation (20% of glomeruli)	Patchy ATN with tubular epithelial sloughing; Intratubular cast formation; Glomerular and small vessel microthrombi
Liver	Moderate portal lymphocytic infiltration & interface hepatitis; Mild bile ductular proliferation; Portal-portal bridging fibrosis; Mild steatosis	Lobular spotty necrosis with neutrophilic microabscess; Sinusoidal dilation; Mild portal inflammation; IHC: CMV negative	Scattered centrilobular necrosis; Mild macro- & micro-vesicular steatosis; Sinusoidal lymphocytic aggregates	Mild macro- & micro-vesicular steatosis; Sinusoidal congestion	Mild macro- & micro-vesicular steatosis; Sinusoidal congestion

DAD, Diffuse alveolar damage; CD, Cluster differentiation; CMV, Cytomegalovirus; IHC, Immunohistochemistry; TTF1, Thyroid transcription factor-1; ATN, Acute tubular necrosis.

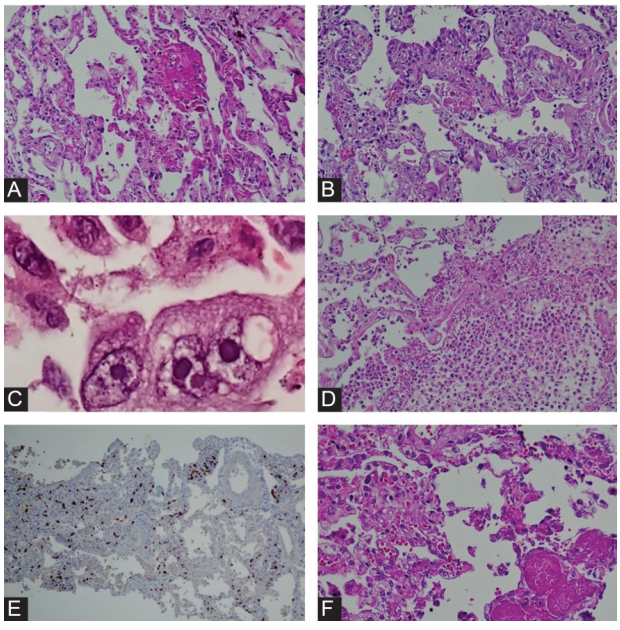

Figure 1. Lung tissue Reveals Alveolar Damage; Pneumocyte Necrosis, Desquamation and Hyperplasia with fibrin Deposition and Interstitial Inflammation H&E Stain, ×400. (A) early interstitial fibrosis and presence of syncytial pneumocytes H&E stain, ×400 (B), CMV-like cytopathic effect of pneumocytes; multinucleated giant cell with intranuclear inclusions and vacuolated cytoplasm H&E stain, ×1000 (C), alveolar neutrophilic infiltration; bacterial superinfection H&E stain, ×400 (D) CD4+ T lymphocytes infiltrating alveolar interstitium, IHC stain for CD4, ×30 (E) and fibrin thrombi in small pulmonary vessels H&E stain, ×400 (F).

hyperchromatic box-car shaped nuclei, representing hypertensive cardiomyopathy.

IHC Findings

Cases 1 and 4: Admixture of CD4+ and CD8+ T lymphocytes, mostly perivascular aggregation (Figure 2).

Kidney

Case 1: Chronic tubulointerstitial nephritis with tubular atrophy (thyroidization), moderate interstitial lymphocytic infiltration and interstitial fibrosis; also, glomerular obsolescence involving nearly 20% of examined glomeruli.

Case 2: Normal renal histology.

Case 3: Acute tubular necrosis superimposed on chronic changes, including focal tubular atrophy, medullary interstitial fibrosis, and focal glomerular obsolescence

Case 4: Acute tubular necrosis and crescent formation in 2 out of 11 glomeruli.

Case 5: Acute tubular necrosis and small vessel fibrin thrombi, mostly in the renal medulla as well as frequent glomerular capillary thrombosis (Figure 3).

Liver

All cases showed sinusoidal dilation, predominantly portal mild to moderate chronic inflammation, sinusoidal congestion and mild mixed macro-, micro-vesicular

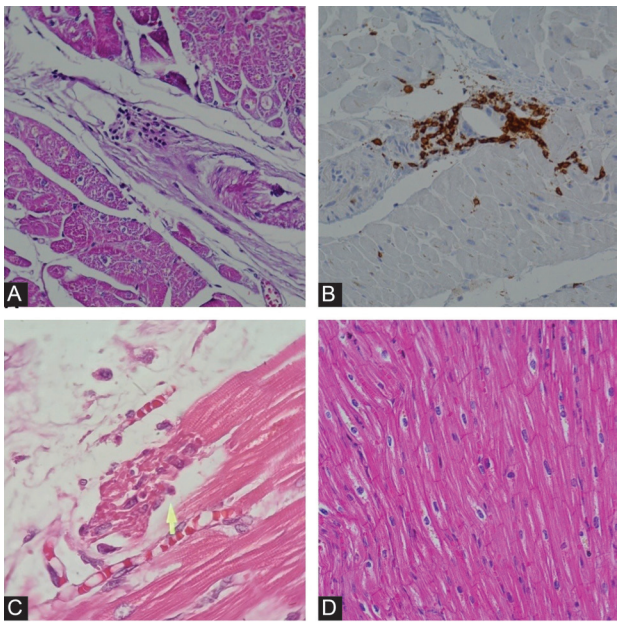

Figure 2. Myocardial Perivascular Inflammation, H&E Stain, ×400 (A), CD8+ T lymphocytes infiltrating Small Vessels, IHC Stain for CD8, ×400 (B), Scattered Single Cell Necrosis, H&E Stain, ×1000 (C), Myocytes with Box-Car Nuclei, H&E Stain, ×400 (D).

steatosis. The additional findings shared by cases 1, 2, and 3 are detailed as follows:

Case 1: Interface hepatitis and portal-portal bridging fibrosis, consistent with chronic hepatitis of grade 3/18, and stage 3/6 based on Ishak classification; these were mainly chronic findings.

Case 2: Lobular multifocal neutrophilic micro-abscess formation like CMV hepatitis. No viral cytopathic effect was identified.

Case 3: Centrilobular necrosis, which may be due to cardiac failure or viral hepatotoxicity (Figure 4).

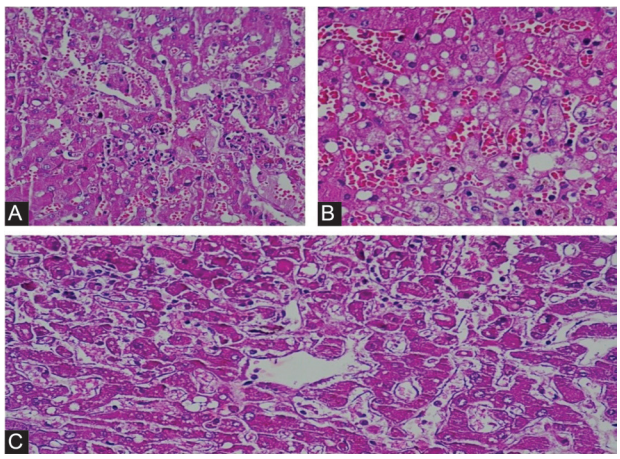

Figure 3. Liver Tissue Shows Lobular Neutrophilic Microabscess Formation and Sinusoidal Congestion (A), Micro-Vesicular Steatosis (B), Lobular Necrosis And Lymphocytic Infiltration (C). A,B,C: H&E stain, ×400..

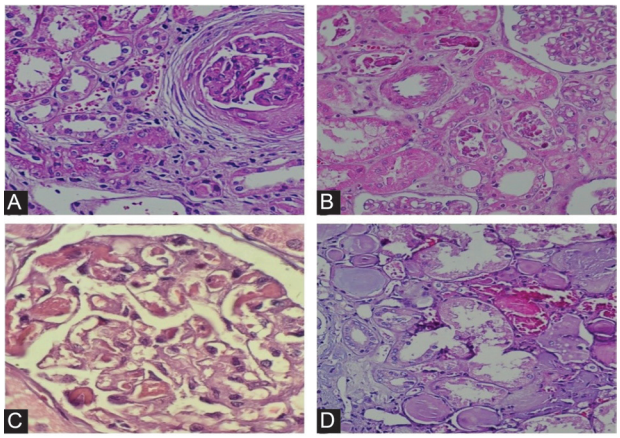

Figure 4. Renal Tissue Exhibits Glomerular Crescent Formation, H&E Stain, ×400. (A) acute tubular damage, H&E stain, ×400, (B) frequent glomerular capillary thrombosis, H&E stain, ×1000, and (C) renal thyroidization in addition to glomerular obsolescence, H&E stain, ×400 (D).

Discussion

This study is a clinicopathologic correlation of five fatal cases of COVID-19 cared for at Loghman Hakim hospital, Tehran, Iran, based on postmortem examination from 4 organs (lung, heart, kidney, and liver). As we do not have any safe autopsy suites to handle highly infective cadavers, we decided to obtain a tissue sample by the ultrasound-guided core needle biopsies rather than a formal autopsy.

The observations in our study contribute further to what we have learned about the pathogenesis of COVID-19 which can improve our clinical approach to the care of these patients. In our opinion, the pathological findings of COVID-19 in our study resemble those of influenza (H1N1), SARS-CoV, and MERS-CoV.[2,3]

As indicated in prior studies, the gross and microscopic characteristics of COVID-19, which initiate mainly in the lungs, lead to pulmonary edema, pulmonary consolidation, increased lung weight, pericarditis and pleuritis. Secondary and co-infections may be superimposed on the viral infection, contributing to purulent inflammation and secretion, which is a characteristic feature of bacterial and/or fungal infections.[4,5]

The remarkable histological findings of lung biopsies were coexistence of all DAD phases, including exudative, proliferative, and fibrotic, suggesting ongoing cycles of lung damage, likely arising from persistent viral replication in the lung tissue and subsequent T cell over-activation and cytokine storms. The presence of micro-thrombi, seen in COVID-19, in the pulmonary microvasculature should be highlighted, which might have resulted from a systemic hypercoagulable state besides being a component of DAD.[6] However, not all DADs lead to a hypercoagulable state.

Furthermore, acute pneumonia which was detected in one of our cases may be presumably representative of superimposed bacterial infection on an underlying SARS-CoV-2 infection.

It should be kept in mind that SARS and COVID-19 infections exhibit common pathogenetic, clinical and pathological findings. Clinically, cough and fever have been the most prominent manifestations of both diseases, while myalgia and diarrhea have been less frequent in COVID-19 cases. Clinically, ARDS has been the most serious pulmonary adverse event that has caused high mortality rates. Histologically, the most common pathology of the non-survivors of either SARS or COVID-19 has been DAD. In previous studies, it was indicated that SARS patients who died with a disease duration under 10-14 days demonstrated acute DAD, while cases with a disease duration surpassing 10-14 days showed the proliferative phase of DAD .[7]

Data is still emerging regarding the routine histopathology of major organs in the autopsies of patients with severe COVID-19. Pathological findings are primarily focused on lung injury and DAD as the cause of death, but there are significant changes in other organs, such as the heart, liver, and kidneys, which require more extensive investigation.[8]

In two of five myocardial samples, perivascular infiltration of T lymphocytes might have played a role in myocardial injury by disrupting microvascular perfusion and/or T lymphocyte cytotoxic effects. Other studies have demonstrated that a small but noticeable percentage of hospitalized patients develop Acute COVID-19 Cardiovascular Syndrome which can occur in the form of several clinical manifestations, such as cardiomyopathy, acute congestive heart failure, ventricular arrhythmias and hemodynamic instability in the absence of significant obstructive coronary artery disease.

The etiological reasons for these defects remain unknown; however, they are believed to be consistent with cardiomyopathy associated with stress, systemic cytokine-mediated microvascular injuries and myocarditis. Although histologically unproven, direct cytopathic effects of SARS-CoV-2 inside cardiomyocytes and pericytes may cause viral myocarditis.

The presence of platelet/fibrin microthrombi in alveolar small vessels, as we noticed in our study and in several newly published articles, has created ambiguity about the significance of this finding, whether this is part of what usually happens in the context of DAD or a systemic coagulopathy dominates in COVID-19 infected patients.[9] This probable coagulopathic pathogenesis became stronger when we found fibrin thrombi in renal small vessels and some glomeruli. Although definite vasculitis was not observed in our examination, it did raise suspicions about viral induced endotheliopathy as mentioned by Varga et al.[10] Prior experience with SARS has helped to investigate possible therapeutic options such as convalescent serum, interleukin-6 inhibitors, and anti-viral drugs for the management of COVID-19.[11]

The central perivenular necrosis and neutrophilic lobular micro-abscess formation, along with sinusoidal lymphocytosis which were identified in the liver biopsy samples, resemble the liver pathology findings in hepatitis provoked by influenza H1N1, CMV or EBV or drug-induced hepatitis. The related micro-vesicular steatosis, arising from acquired cellular oxidative defects, can also be a detrimental prognostic feature.[4,12] Accordingly, other related studies have observed micro-vesicular steatosis with moderate inflammation within the liver; it has been deemed uncertain if this is due to the virus itself or caused by iatrogenic factors. These characteristics are remarkably close to those seen in SARS and MERS-coronavirus infection. The crescent seen on the renal biopsy samples of our patient may have been the upshot of viral infection or accompanying cytokine storm. The majority of renal biopsies in our study displayed signs of acute tubular injury with necrosis and flattening of tubular epithelium, multiple tubular casts and interstitial edema in some patients superimposed on chronic changes such as interstitial nephritis and tubular atrophy (thyroidization). These findings are similar to other studies and in favor of susceptibility of patients with chronic kidney disease to severe COVID19 infections.[13] However, ischemic ATN may have been the result of systemic coagulopathy or fatal systemic hypotension, compounded by the chronic pathological findings of chronic tubulointerstitial nephritis, tubular atrophy, and glomerular obsolescence which might have contributed to the severe renal injury and patient demise.[1,14]

In conclusion, regarding the histopathological autopsy findings of fatal COVID-19 patients in our small case series, the lung samples indicated that the three DAD phases (exudative, proliferative and fibrotic) can be present simultaneously, delineating ongoing cycles of lung damage, which could be explained by tenacious viral replication and T cells over-activation, along with cytokine storms. Also, superimposed bacterial infection could be a possibility, according to one incidence of acute pneumonia in our study. Additionally, the perivascular infiltration of T lymphocytes which we observed in the myocardial tissue showed T lymphocyte cytotoxic effects and disruption of microvascular perfusion which could be a significant underlying cause of myocardial failure. Moreover, findings from other organs like the liver and kidneys were suggestive of acquired cellular oxidative defects, necrosis, micro-abscess formation, tissue atrophy, and coagulopathy. Our pathological findings which are associated with poor prognosis highlight the importance of prognostic significance drawn from the histopathology in patients with COVID-19.

Authors' Contribution

FBZ and SS making pathologic photos and drafted the manuscript. HBM, MA and MH have participated in sampling. IAD Participated

in research design and writing of the paper. Also managed the project and select the cases. IAD, MM, MMR, SSNI, FET, PTN and BM revised and edited the article. OM participated as study advisor. All authors read and approved the final manuscript.

Conflict of Interest Disclosures

The authors declare that there is no conflict of interest.

Ethical Statement

The study was approved by the Ethics in Medical Research Committee of the Shahid Beheshti University of Medical Sciences with an Aapproval number of IR.SBMU.RETECH.REC.1399.057 on 20th April 2020, and is accessible online at: http://ethics.research.ac.ir/ProposalView.php?id=130327 (English version: http://ethics.research.ac.ir/form/4831gtq9g9e9aeyj.pdf).

Acknowledgements

The authors would like to thank the Clinical Research Development Unit (CRDU) of Loghman Hakim Hospital, Shahid Beheshti University of Medical Sciences, Tehran, Iran for their help and support in conducting this clinical trial.

References

1. Duncanson ER, Mackey-Bojack SM. Histologic Examination of the Heart in the Forensic Autopsy. Acad Forensic Pathol. 2018;8(3):565-615. doi: 10.1177/1925362118797736.
2. Ding Y, Wang H, Shen H, Li Z, Geng J, Han H, et al. The clinical pathology of severe acute respiratory syndrome (SARS): a report from China. J Pathol. 2003;200(3):282-9. doi: 10.1002/path.1440.
3. Balraam KVV, Sidhu A, Srinivas V. Interesting post-mortem findings in a H1N1 influenza-positive pneumonia patient. Autops Case Rep. 2019;9(2):e2018079. doi: 10.4322/acr.2018.079.
4. Hanley B, Lucas SB, Youd E. Autopsy in suspected COVID-19 cases. J Clin Pathol. 2020;73(5):239-42. doi: 10.1136/jclinpath-2020-206522.
5. The Royal College of Pathologists. Autopsy practice relating to possible cases of COVID-19 (2019-nCov, novel coronavirus from China 2019/2020). 2020. Available from: https://www.rcpath.org/uploads/assets/d5e28baf-5789-4b0f-acecfe370eee6223/447e37d0-29dd-4994-a11fe27b93de0905/Briefing-on-COVID-19-autopsy-Feb-2020.pdf.
6. Broaddus VC, Mason RJ. Murray & Nadel's Textbook of Respiratory Medicine. 6th ed. Philadelphia: Elsevier Saunders. 2016.
7. Zhang T, Sun LX, Feng RE. Comparison of clinical and pathological features between severe acute respiratory syndrome and coronavirus disease 2019. Zhonghua Jie He He Hu Xi Za Zhi. 12;43(6):496-502. doi: 10.3760/cma.j.cn112147-20200311-00312.
8. Barton LM, Duval EJ, Stroberg E, Ghosh S, Mukhopadhyay S. Covid-19 autopsies, oklahoma, usa. Am J Clin Pathol. 2020;153(6):725-33. doi: 10.1093/ajcp/aqaa062.
9. Varga Z, Flammer AJ, Steiger P, Haberecker M, Andermatt R, Zinkernagel AS, et al. Endothelial cell infection and endotheliitis in COVID-19. Lancet. 2020;395(10234):1417-8. doi:10.1016/S0140-6736(20)30937-5.
10. Hendren NS, Drazner MH, Bozkurt B, Cooper LT Jr. Description and Proposed Management of the Acute COVID-19 Cardiovascular Syndrome. Circulation. 2020;141:1903–14. doi: 10.1161/circulationaha.120.047349.
11. Tandra S, Yeh MM, Brunt EM, Vuppalanchi R, Cummings OW, Ünalp-Arida A, et al. Presence and significance of microvesicular steatosis in nonalcoholic fatty liver disease. J Hepatol. 2011;55(3):654-9. doi: 10.1016/j.jhep.2010.11.021.
12. Ng DL, Al Hosani F, Keating MK, Gerber SI, Jones TL, Metcalfe MG, et al. Clinicopathologic, immunohistochemical, and ultrastructural findings of a fatal case of Middle East respiratory syndrome coronavirus infection in the United Arab Emirates, April 2014. Am J Pathol. 2016;186(3):652-8. doi: 10.1016/j.ajpath.2015.10.024.
13. Menter T, Haslbauer JD, Nienhold R, Savic S, Hopfer H, Deigendesch N, et al. Post-mortem examination of COVID19 patients reveals diffuse alveolar damage with severe capillary congestion and variegated findings of lungs and other organs suggesting vascular dysfunction. Histopathology. 2020;77(2):198-209. doi: 10.1111/his.14134.
14. Schrier RW, Shchekochikhin D, Ginès P. Renal failure in cirrhosis: prerenal azotemia, hepatorenal syndrome and acute tubular necrosis. Nephrol Dial Transplant. 2012;27(7):2625-8. doi: 10.1093/ndt/gfs067.